NIH Public Access
Author Manuscript
Biochim Biophys Acta. Author manuscript; available in PMC 2015 October 01.

Published in final edited form as:
Biochim Biophys Acta. 2014 October ; 1838(10): 2511–2519. doi:10.1016/j.bbamem.2014.05.024.

Ceramide – Lipid Interactions studied by MD Simulations and Solid-State NMR

Bercem Dutagaci[†], **Johanna Becker-Baldus**[†], **José D. Faraldo-Gómez**[‡], and **Clemens Glaubitz**[†,*]

[†]Institute of Biophysical Chemistry, J.W. Goethe-University, Max-von-Laue-Str. 9, 60438 Frankfurt, Germany

[‡]Theoretical Molecular Biophysics Section, National Heart, Lung & Blood Institute, National Institutes of Health, Bethesda, MD 20892, USA

Abstract

Ceramides play a key modulatory role in many cellular processes, which results from their effect on the structure and dynamics of biological membranes. In this study, we investigate the influence of C16-ceramide (C16) on the biophysical properties of DMPC lipid bilayers using solid-state NMR and atomistic molecular dynamics (MD) simulations. MD simulations and NMR measurements were carried out for a pure DMPC bilayer and for a 20% DMPC-C16 mixture. Calculated key structural properties, namely area per lipid, chain order parameters, and mass density profiles, indicate that C16 has an ordering effect on the DMPC bilayer. Furthermore, the simulations predict that specific hydrogen-bonds form between DMPC and C16 molecules. Multi-nuclear solid-state NMR was used to verify these theoretical predictions. Chain order parameters extracted from ^{13}C-^{1}H dipole couplings were measured for both lipid and ceramide and follow the trend suggested by the MD simulations. Furthermore, ^{1}H-MAS NMR experiments showed a direct contact between ceramide and lipids.

Keywords

Ceramide; DMPC; MAS NMR; MD simulations; lipid rafts

Introduction

Ceramides are important bioactive sphingolipids that act as second messengers in cell signal transduction [1, 2]. Hence, they play important roles in facilitating and modulating many cell processes including apoptosis, differentiation, and senescence [3-6]. The mechanism that underlies the physiological role of ceramides has not been completely clarified yet, and

© 2014 Elsevier B.V. All rights reserved.

[*]Correspondence should be addressed to: Prof. Dr. Clemens Glaubitz,, Institute of Biophysical Chemistry, J.W. Goethe-University, Max-von-Laue-Str. 9, 60438 Frankfurt, Germany, Tel: +49 (0)69 79829927, Fax: +49 (0)69 79829929, glaubitz@em.uni-frankfurt.de.

Publisher's Disclaimer: This is a PDF file of an unedited manuscript that has been accepted for publication. As a service to our customers we are providing this early version of the manuscript. The manuscript will undergo copyediting, typesetting, and review of the resulting proof before it is published in its final citable form. Please note that during the production process errors may be discovered which could affect the content, and all legal disclaimers that apply to the journal pertain.

NIH-PA Author Manuscript
NIH-PA Author Manuscript
NIH-PA Author Manuscript

NIH-PA Author Manuscript

NIH-PA Author Manuscript

NIH-PA Author Manuscript

thus remains a subject of active research. Recent studies have indicated that this modulatory role is related to the effect that ceramides have on cellular membranes, especially in regard to lipid rafts [7]. Rafts are rigidified membrane domains, formed by clustering of sphingomyelin with cholesterol. In these rafts, cholesterol fills the hydrophobic space inside the sphingomyelin bilayer, resulting in a more compact membrane [8]. Several studies have indicated that in the course of signal-transduction processes rafts become larger and enriched in ceramide, as a result of the hydrolysis of sphingomyelin, catalysed by the enzyme sphingomyelinase (SMase) [9]. These domains are thought to diffuse dynamically along the membrane, and form larger macro-domains called ceramide-enriched platforms. It has been proposed that ceramide macro-domains are important to help receptors to transmit signals across the membrane [10-13].

Ceramides have a fatty-acid chain that is connected to a sphingosine base by an amide bond. The fatty-acid chain lengths found in nature vary from 2 to 28 carbon atoms, in both saturated and unsaturated forms. Short-chain ceramides contain acyl chains with less than 8-10 carbon atoms, while long-chain ceramides may consist of more than 10-12 carbons [14, 15]. Free ceramides occur mainly in the stratum corneum [16], which is the outermost layer of the skin. They are also found in membranes in small amounts, as metabolites or precursors of other compounds [1, 2]. Several published studies have investigated how ceramides behave and organize themselves in membranes [14, 17-26]. Lateral phase separation into a ceramide-dominated gel and a phospholipid-dominated liquid crystalline phase has been observed in some cases [17, 18, 26]. Studies on cell cultures have also indicated that ceramides located in cell membranes can form domains [19].

Several methods have been applied to understand the influence of ceramides on the physical properties of lipid bilayers. Studies based on the fluorescence anisotropy have indicated that phospholipids tend to be more ordered in the presence of ceramides [20, 23, 25]; similar observations have been made using NMR, specifically for ceramides with 16-carbon chains, or C16-ceramide, in DPPC and POPC bilayers [21, 22, 27].

The latter studies indicated that C16 induces a phase separation only in the gel phase; above the lipid main phase transition, C16 diffuses into the phospholipid bilayer and promotes the ordering of the lipid chains. This ordering effect has also been observed in molecular dynamics (MD) simulations of POPC-C16 mixtures [24]. Studies based on both NMR and MD simulations have therefore shown that C16 influences the physical properties of several phospholipid membranes. However, not much is known about the direct interactions formed between lipids and C16.

Here, we characterize the effect of C16-ceramide on DMPC lipid bilayers. DMPC is a saturated phospholipid with 14 carbon atoms in each fatty-acid chain (Fig. 1a). This makes DMPC a good match for C16 (Fig. 1a). DMPC is also often used as a model lipid in solid-state NMR studies, and has been extensively characterized. Therefore this lipid type is an ideal choice for ceramide-lipid interaction studies. Furthermore, C16 is known to be one of the main components of the natural ceramide pool [2]. Our methodological approach is based on atomistic MD simulations, by which we gain specific insights that are verified and expanded by solid-state NMR experiments. In the following, we show that C16 causes a

NIH-PA Author Manuscript

NIH-PA Author Manuscript

NIH-PA Author Manuscript

significant ordering effect on DMPC membranes, which is caused by the formation of H-bonded C16-DMPC complexes dissolved within fluid lipid bilayers. Experimental evidence derives from ^{1}H-MAS-NMR, and ^{1}H-NOESY-MAS measurements, as well as from the determination of dipolar C-H order parameters.

Materials and Methods

Sample Preparation

1,2-dimyristoyl-*sn*-glycero-3-phosphocholine (DMPC), 1,2-dimyristoyl-d54-*sn*-glycero-3-phosphocholine-1,1,2,2-d4-N,N,N-trimethyl-d9 (DMPC-d_{67}) and N-palmitoyl-D-*erythro*-sphingosine (C16-ceramide; C16) were obtained from Avanti Polar Lipids and used without further purification. Liposome samples were prepared following standard procedures [28]. The appropriate amounts of DMPC and C16 (usually 20:4 mg/mg) were co-dissolved in chloroform (5 mL) and shaken until a clear solution was obtained. The bulk solvent was evaporated under a stream of nitrogen gas and subsequently dried overnight in a rotary evaporator under high vacuum, resulting in a dry lipid-substrate film. Samples were rehydrated slowly inside a round-bottom flask by adding 1 mL of water under slow rotation until a multi-lamellar dispersion was formed. Hydrated samples were transferred to an Eppendorf tube and pelleted by centrifugation for one hour at 16060 g. Bulk water was removed and samples were dehydrated by lyophilisation followed by another rehydration step through direct addition of 10 μL of water. In our experience, this additional step, which hydrates the bilayer sufficiently but avoids bulk water, is required to obtain the best-resolved MAS-NMR spectra of lipid vesicles. Four freeze-thaw cycles were performed between temperatures that were below and above the transition temperature of the lipids, to obtain more homogeneous liposomes. Finally, samples were transferred to a Bruker 3.2 mm MAS-NMR rotor.

MD Simulations

A pure DMPC bilayer and a DMPC bilayer containing 20% C16 were simulated for a total of 100 ns each. The pure DMPC bilayer consisted of 128 lipids and 3655 water molecules. Initial coordinates were kindly provided by Tieleman et al. (http://wcm.ucalgary.ca/tieleman/downloads). To model the mixed bilayer, 26 DMPC molecules were randomly chosen after a 10 ns equilibration of the pure bilayer, and replaced by ceramide molecules. The initial position of the ceramide molecules in the bilayer was such that their centres of mass coincided with those of the replaced DMPC lipids. Energy minimizations were used to remove steric clashes prior to the molecular dynamics simulation.

The force-field parameters used for DMPC are those developed by Berger et al. [29]. For the ceramide acyl chains, we adapted the bonded and non-bonded interaction parameters used for DMPC, and for the ceramide head group we adapted parameters for equivalent chemical groups from the GROMOS87 protein force-field (Fig. S1) [30]. The SPC water model was used. All simulations were performed using GROMACS 4.0.3 [30] using LINCS to constraint bond-lengths involving hydrogen atoms.

NIH-PA Author Manuscript

NIH-PA Author Manuscript

NIH-PA Author Manuscript

Periodic boundary conditions were applied in three dimensions. Short-range Coulomb and van-der-Waals interactions were cut-off at 11 Å. The Particle-Mesh-Ewald algorithm was used to calculate long-range electrostatic interactions (no dispersion correction were used). Neighbor lists were updated every 5 integration steps using the grid method. Both simulations were carried out at a temperature of 310 K (i.e. above the DMPC gel-to-liquid crystalline transition temperature of ∼297 K) and 1 bar of pressure, using the Nosé-Hoover thermostat and a semi-isotropic Parrinello-Rahman barostat. The time constants of the thermostat and barostat were 0.1 and 1 ps, respectively.

From the MD trajectories it is possible to quantify several observables that characterize the structure and dynamics of the membrane. Bilayer widths and mass-density profiles, carbon-hydrogen (C-H) order parameters, and hydrogen-bonding patterns between ceramide and lipid molecules were analysed using standard tools available in GROMACS 4.0.3 [30], using the last 90 ns of each simulation. To calculate the area per lipid, we employed a methodology based on the tessellation of each monolayer into Voronoi cells [31], at each simulation snapshot, on account of the fact that ceramide and lipids occupy different volumes. Following Pandit et al. [32], we used the XY coordinates of three specific atom types per lipid/ceramide molecule to perform a Delaunay triangulation [33]. The atoms selected represent the location of the acyl tails and the head group of both DMPC and ceramide. For C16, these atoms are C2′, C3′ and C1″; for DMPC, we used C1 in both chains and Cg2 in the glycerol backbone. By combining the set of triangles assigned to each of the atoms in a given molecule, Voronoi polygons for that molecule were then obtained, whose total area is the area covered by that molecule at that particular time-point in the simulation. This analysis thus results in a set of molecular areas for each monolayer and for each simulation snapshot, which were combined and are represented as probability distributions (Fig. 3). To reduce boundary artefacts, the Delaunay triangulation was carried out on an extended simulation box that includes periodic images in both ±X and ±Y directions. Delaunay triangles and Voronoi diagrams were calculated using Triangle [34]. A Python script was developed to calculate areas and probability distributions.

Solid State NMR

All experiments were carried out using a Bruker Avance III 850 WB spectrometer operating at a proton Larmor frequency of 850 MHz. A Bruker 3.2mm MAS HCN probe head was used for all measurements. Dipole order parameters were determined by separated local field spectroscopy based on PISEMA as described by Sandström and co-workers [35, 36] using amplitude modulated FSLG-CP during t_1. For FSLG-CP, a 42 kHz ^{1}H field was used. Spectra were recorded at 10 kHz sample rotation rate with 4096 points in the chemical shift and 256 points in the dipolar dimension. A recycle delay of 3 s was used. Proton decoupling during acquisition was 80 kHz. Dipole couplings were determined by correcting the observed dipolar splittings by the FSLG scaling factor (0.577 for CH, 0.816 for CH_2). The order parameters (S_{CH}) were calculated from the ratio between measured and static dipole couplings (21.5 kHz for single C-H bond [35]. ^{1}H NMR spectra were recorded using 10 kHz sample rotation rate, 51 ms acquisition time and 10 kHz bandwidth and a recycle delay of 3 s. For ^{1}H-MAS NOESY (Nuclear Overhauser effect spectroscopy), a bandwidth of 17 kHz for both direct and indirect dimensions was used. Signal acquisition was carried out by the

NIH-PA Author Manuscript

NIH-PA Author Manuscript

NIH-PA Author Manuscript

TPPI method with acquisition times of 40 ms for direct and 15 ms for indirect dimensions. Proton chemical shift referencing was done internally for each spectrum with respect to TMS via the terminal methyl group of the lipid chains at 0.89 ppm. A temperature calibration under MAS-NMR conditions was carried out by observing the known phase transition of DMPC in ^{1}H-MAS NMR spectra (Fig. S2).

Results

(a) MD Simulations

To investigate the effects of C16 on DMPC bilayers at the molecular level, we carried out MD simulations of a pure DMPC bilayer as well as of a DMPC bilayer that contains 20% ceramide. After 100 ns of simulation, snapshots of both systems revealed apparent differences in the structure of the two membranes, as illustrated in Fig. 1b. In the presence of ceramide, DMPC molecules seem to be more closely packed and the bilayer appears to be thicker. To characterize and rationalize this change, we quantified the influence of C16 on the area per lipid, the mass-density profile along the membrane normal, the acyl-chain order parameters and the inter-molecular hydrogen-bonding pattern. These results are summarized in Table 1.

Area per Lipid—To calculate the area per lipid, we used a Voronoi tessellation method based on a Delaunay triangulation, to account for the fact that DMPC and C16 do not occupy the same volume (see Materials and Methods). The outcome of this calculation is a time-series of area values for each molecule in each monolayer, from which a global average and a probability distribution for either molecule type can be obtained. In Fig. 2a we compare these probability distributions for the pure and mixed bilayers. For the pure DMPC, the calculated area per lipid is 61.1 Å^2, in good agreement with the value of 60.6 Å^2 reported by Kucerka et al. [37]. For the DMPC-C16 mixture, the area per lipid for DMPC dropped to 51.0 Å^2. The area per ceramide was also calculated for the mixture, and it was found to be 40.3 Å^2. Thus, replacement of DMPC lipids by ceramide molecules not only decreases the total area of the membrane patch because ceramide requires a smaller area per molecule, but also because it diminishes the area occupied by the DMPC lipids, on average. Altogether, the effect of ceramide is a membrane bilayer that is significantly more densely packed.

Bilayer Width—Fig. 2b shows mass-density profiles along the perpendicular of membrane plane, both for the complete atomic system as well as for water only, extracted from the simulations of the pure DMPC bilayer and the DMPC-ceramide mixture. Like the area-per-lipid data, these profiles are obtained for each snapshot in the simulated trajectory, and subsequently time-averaged. Both profiles feature two density peaks, which reflect the extent of the head-group region in each leaflet. The bilayer width can be therefore defined by the distance between these two peaks. It is clear from Fig. 2b that the width of the mixed bilayer is considerably greater than that of the pure DMPC membrane. Specifically, the calculated width of the pure bilayer is 32.3 Å, while for the mixture this value increased to 40.0 Å. This increase in bilayer thickness is consistent with the reduction in the area-per-lipid, which logically results in an elongation the volume occupied by each molecule.

NIH-PA Author Manuscript

NIH-PA Author Manuscript

NIH-PA Author Manuscript

Chain Order Parameters—Lipid order parameters provide information about the anisotropy in the arrangement of the acyl chains, which is related to their mobility. These order parameters are averages over time and over molecules of the same type, and are generally derived for each carbon atom along the chain, from the angle of the corresponding C-H bond with respect to the bilayer normal. Values closer to 0 reflect greater isotropy and therefore greater mobility, while values closer to 1 reflect ordering of the acyl chains in configurations parallel to the bilayer normal. Fig. 3 shows the calculated order parameters for the two acyl chains of DMPC in each simulation system, as well as for the acyl and sphingosine chains of ceramide in the mixed bilayer. It is apparent that the ordering of the hydrocarbon chains in DMPC increases in the presence of ceramide. The order parameters of the two ceramide chains are similar, and greater than the order parameters of the DMPC chains in the pure lipid bilayer, which are also similar to each other. However, in the mixed bilayer the ordering of the DMPC chain increases markedly. These data are consistent with the above-mentioned reduction in the area-per-lipid and the thickening of the membrane as a result of the introduction of ceramide.

Hydrogen-Bonding Interactions—The pronounced effect of C16 on the DMPC bilayer raises the question of whether specific interactions between these two molecule types occur. To address this question, we analysed the formation of persistent hydrogen bonds between C16 and DMPC molecules in the simulated mixed bilayer. Potential H-bond donors in C16 (D1/NH, D2/1-OH, D3/3-OH) and acceptors in DMPC (A1-A8) are shown in Fig. 4a. All possible donor-acceptor interactions were monitored individually. To quantify the likelihood of a particular H-bond, we annotated whether that bond was formed or not in each of the snapshots of the simulated trajectory, and then calculated a time averaged number of H-bonds. The results are shown in Fig. 4b. The data show that the three donors in C16 form H-bonds almost constantly, but not all acceptors in DMPC contribute equally. The first hydroxyl group in the sphingosine chain (D2) forms H-bonds primarily with accepting oxygen atoms in the DMPC phosphate head-group (A8) whereas the amide (D1) and the second hydroxyl group (D3) form H-bonds typically with the carbonyl oxygen atoms in the glycerol backbone of the DMPC chains. The most likely H-bonds, e.g. defined as those exceeding a probability threshold of 0.2, are between A1 and D1/D2/D3, A2 and D1, A3 and D1, and A8 and D2 (highlighted in Fig. 4a). Especially A1-D3 (O$\overset{\cdot\cdot}{H}$O) and A8-D2 (O$\overset{\cdot\cdot}{H}$O) were observed to be highly populated.

The occurrence of water-DMPC, water-C16, and C16-C16 H-bonds was also analysed. On average, a given C16 molecule accepts only one H-bond donated by water, despite the fact that it has four potential acceptors (three of which are also donors). The number of hydrogen bonds between C16 molecules was negligible, consistent with the fact that no ceramide clusters or domains were formed within the time-scale of the simulation (the distribution of pairwise distances between C16 molecules is centred around 25 Å). Interestingly, the simulations indicate that the hydrogen bonds formed between C16 and DMPC do not disturb the interactions of DMPC with water drastically. DMPC molecules have no hydrogen bond donors, only acceptors. Therefore, hydrogen bonds between DMPC molecules were not observed. However, for pure DMPC, on average 6 of the 9 possible acceptors were engaged

NIH-PA Author Manuscript

NIH-PA Author Manuscript

NIH-PA Author Manuscript

in H-bonds donated by water molecules. In the DMPC-C16 mixture, this number decreased only slightly, to about 5.5 H-bonds per DMPC molecule.

In summary, analysis of hydrogen-bonding patterns in the mixed bilayer simulation underscores the existence of persistent close-range interactions between both the head groups and the chains of C16 and DMPC, explaining the noticeable effect of C16 on the order parameters of the DMPC acyl chains, and thus on the morphology of the membrane.

(b) Solid-State NMR

The MD simulations outlined above predict an increase in lipid order in the presence of ceramide and also specific lipid-ceramide interactions. Here, solid-state NMR is applied to verify these findings.

^{13}C-^{1}H Dipolar Order Parameters—Lipid and ceramide order parameters were determined by ^{13}C-^{1}H dipolar separated local field spectroscopy based on the PISEMA experiment [35, 36]. Spectra recorded at 325 K are shown in Fig. 5. At this temperature, both C16 and DMPC are in a fluid phase within the mixture as visible from ^{1}H-MAS NMR spectra (see below). Order parameters S_{CH} were calculated from the dipole splittings and are plotted against the corresponding carbon position to yield an order parameter profile (Fig. 5D). In the presence of 20% C16, the lipid chain order increases (for carbons 4-11 from 0.25 to 0.29), while glycerol backbone and headgroup are unaffected. The order parameter of the acyl chain of C16 itself was determined by replacing DMPC with DMPC-d_{67}. In this sample, only dipole splittings from protonated C16 are visible (Fig. 5C). Their order parameters are similar to those of DMPC in the mixed bilayer. These data confirm the trend observed in the MD simulations (Fig. 3). C16 has an ordering effect on DMPC, but the chain order of both C16 and DMPC in the mixed bilayer is smaller than that observed in the simulations (Fig. 3).

^{1}H-MAS NMR—To further disentangle the effect of C16 on DMPC lipid bilayers, temperature dependent ^{1}H-MAS NMR spectra were recorded (Figs. 6 and S2). The main lipid phase transition can be conveniently derived from the lipid CH_2 resonance, which shows severe broadening due to strong ^{1}H-^{1}H dipole couplings in the gel phase, but narrows remarkably in the liquid crystalline phase due to fast rotational diffusion and trans-gauche isomerization. Upon addition of 20% C16, the DMPC phase transition raises by 10 K from around 300 to 310 K (Fig. S2). As noted previously [38], C16-ceramide alone shows a much higher phase transition around 370 K (Fig. 6a), which decreases to around 320 K in the mixed bilayer, which is close but not identical to the DMPC phase transition temperature (Fig. 6c). Here, deuterated DMPC-d_{67} was used in order to make the C16 protons better visible in the mixture. In this sample, only glycerol backbone protons g1, g2 and g3 remain protonated (Fig. 6b). The proton spectra of the DMPC-d_{67}/C16(20%) mixture are in principle a superposition of the individual C16 and DMPC-d_{67} spectra, but one additional resonance at 3.25 ppm (labelled A in Fig. 6c) occurs.

Based on our MD simulations, we predicted potential H-bond formation between C16 and DMPC involving NH and OH groups in C16 as proton donors (Fig. 4). In order to observe these exchangeable sites, experiments in H_2O and D_2O were carried out (Fig. 6d). The NH

NIH-PA Author Manuscript

NIH-PA Author Manuscript

NIH-PA Author Manuscript

proton is observed in both C16 and DMPC-d_{67}/C16 (20%) in H_2O at 6.8 ppm but disappears in D_2O. In contrast, resonance A is only observed in the mixture under both H_2O and D_2O conditions. For deuterium exchange experiments, samples were first measured in H_2O followed by solvent exchange. This resonance is tentatively assigned to an OH proton. OH protons are usually difficult to observe due to exchange with bulk water. However, exchange can be slowed down by several orders of magnitudes if the proton is involved in a hydrogen bond. In organic solvent, OH of C16 was detected at 2.7 ppm [39]. The chemical shift observed here at 3.25 ppm, the fact that it only occurs in the mixture and that it is observed in both D_2O and H_2O indicates that this proton is involved in a H-bond with DMPC.

To probe for direct C16-DMPC interactions, ^{1}H-NOESY MAS NMR spectra of DMPC-d_{67}/C16 (20%) were recorded. This method has been shown to offer valuable insight into intermolecular interactions within fluid lipid bilayers [40]. A series of NOESY spectra at different temperatures above 300K and mixing times between 50 and 1000 ms were recorded. As seen in Fig. 6e, cross-peaks between A and C16 as well as DMPC protons are observed at 310 K and 200 ms mixing time. Unfortunately, the remaining protons g1, g2 and g3 of DMPC-d_{67} partially overlap with the C16 protons under these conditions. To reduce spectral overlap, a temperature of 340 K was chosen at which DMPC and C16 resonances are better separated (Figs. 6 & Fig. 7a). Here, unambiguous intermolecular correlations between g1 and g2 in DMPC and a number of ceramide protons are observed at long mixing times (1000 ms). This long mixing time was needed to observe long-range intermolecular contacts. Unfortunately, cross-peaks between A and C16 and DMPC are much reduced under these conditions, but our data show clearly through-space contacts between DMPC and C16 compatible with the H-bonding pattern observed in the simulations.

Discussion

Ceramides are known to play an important role in many cell processes. They induce the formation of macro-domain platforms from rafts and consequently act as second messengers in cellular signal transduction [1, 2, 9]. This role has been attributed to their effect on the physical properties of cell membranes [7]. Several studies have shown that ceramides induce lateral phase separation in lipid membranes into ceramide-assisted gel phase and phospholipid-assisted liquid-crystalline phases [17-19, 26]. It was also shown that ceramides have a large effect on order parameters of phospholipid chains [20-25]. Fluorescence polarization studies predicted that ceramides increase the order of phospholipids [20, 23, 25] and ^{2}H NMR studies showed the effects on segmental order parameters [21, 22].

The aim of this study was to probe the effect of C16-ceramide on DMPC lipid bilayers using MD simulations, and to verify the computational findings by solid-state NMR. Our simulations show a strong ordering effect of C16 on DMPC, indicated by a reduction in the average area per lipid (Fig. 2a), increased bilayer thickness (Fig. 2b) and increased chain order parameters (Fig. 3). These findings are in qualitative agreement with the NMR measurements, which also reveal a clear ordering effect (Fig. 5). The extent of this effect, however, is more pronounced in the simulations than in the experiment (Fig. S3). For example, the measured change in the DMPC order parameters in the presence of C16, interpreted via the diamond-lattice model [41] would imply a reduction in the area per lipid

NIH-PA Author Manuscript

NIH-PA Author Manuscript

NIH-PA Author Manuscript

of about 4 $Å^2$; the value computed directly from the simulation is about 10 $Å^2$. However, given the fact that the force-field parameters used for C16 were not specifically optimized to reproduce any experimental data, this quantitative discrepancy is not unexpected.

The simulations reveal no significant orientational bias on the DMPC head-groups induced by ceramide at the concentration studied (20%). For example, the characteristic tilt-angle of the P-C_{g2} vector in the DMPC head-group relative to the membrane normal changes from 31.1° in pure DMPC to 30.0° in the mixture, indicating that at low ceramide concentrations the mechanism of perturbation of the bilayer does not primarily involve the lipid head-groups. We cannot rule out, however, that the lipid head-groups will also be perturbed in mixtures richer in ceramide. Indeed, an earlier simulation study of the effect of ceramide on sphingomyelin (SM) bilayers shows significant changes in the SM head-group tilt-angle when the ceramide fraction is 50% or greater [42].

Instead, our simulations indicate that H-bonds between C16 and DMPC are the primary interaction mechanism between these species (Fig. 4); consistently, the NOESY data demonstrates unambiguous contacts between C16 and DMPC (Fig. 7). Intermolecular hydrogen-bonding is thought to be an important factor for the formation of phospholipid-sphingolipid complexes [43], but previous studies have not provided strong evidence for this type of interactions between ceramides and phospholipids. Several studies, though, have indicated that hydrogen-bonds occur between ceramide and water and ceramide itself [39, 44, 45], as well as between ceramide and sphingomyelin [42, 46]. For example, the abovementioned simulation study of ceramide-enriched sphingomyelin bilayers [42] reported a pattern of H-bonds between the ceramide NH donor (D1 in Fig. 4) and the oxygen atoms in the sphingosine backbone comparable to what we observe here for DMPC (at a comparable ceramide concentration). The observed H-bonds donated by SM to ceramide, however, cannot be formed by DMPC, which has no donors. In our simulations we observe instead H-bonding interactions mediated by the hydroxyl groups in ceramide (D2 and D3), consistent with the measured NMR peaks for 1-OH and/or 3-OH arising in the mixed bilayer (Fig. 6).

Previous ^{2}H-solid state NMR studies have shown a chain ordering effect of C16 on DPPC [22] and POPC [21] as observed here for DMPC. For DPPC and DMPC, lateral phase separation below or close to the main phase transitions has been suggested [22, 47]. Our ^{1}H-MAS-NMR experiments of DMPC/C16 mixtures (Figs. 6, S2) show slightly different phase transition temperatures for DMPC and C16 within the mixture and a broad phase transition profile for C16 in agreement with earlier reports [48]. Furthermore, order parameter measurements between 310 K and 325 K indicate complex phase behaviour (data not shown). These observations are compatible with a model in which lateral phase separation around the main phase transition temperature occurs, but our data also show that C16 starts to diffuse from a separate gel-like phase into the liquid-crystalline phase of DMPC above the phase transition temperature of 310 K, and is completely dissolved in the fluid phase above 320 K. Our results show that ceramide has a pronounced effect on the physical properties of the DMPC bilayer. Specifically, simulations and NMR show that ceramide increases the rigidity of the DMPC bilayer by increasing the ordering of the lipid acyl chains. Even though the simulations appear to overestimate the strength of the C16-DMPC

NIH-PA Author Manuscript

NIH-PA Author Manuscript

NIH-PA Author Manuscript

interactions, the NMR measurements confirm that C16 and lipids form persistent H-bonding interactions. We therefore propose that the formation of transient complexes between ceramide and DMPC molecules, sustained by close-range hydrogen-bonding interactions, underlies the morphological effect of ceramide on DMPC bilayers.

Supplementary Material

Refer to Web version on PubMed Central for supplementary material.

Acknowledgments

This work was funded by the Center for Biomolecular Magnetic Resonance (BMRZ), the Lipid Signaling Forschungszentrum Frankfurt (Liff) and was supported in part (JDF-G) by the Intramural Research Program of the NIH, NHLBI.

References

1. Futerman AH, Hannun YA. The complex life of simple sphingolipids. Embo Reports. 2004; 5:777–782. [PubMed: 15289826]
2. Kolesnick RN, Goni FM, Alonso A. Compartmentalization of ceramide signaling: Physical foundations and biological effects. J Cell Physiol. 2000; 184:285–300. [PubMed: 10911359]
3. Hannun YA, Obeid LM. The ceramide-centric universe of lipid-mediated cell regulation: Stress encounters of the lipid kind. J Biol Chem. 2002; 277:25847–25850. [PubMed: 12011103]
4. Kolesnick R. The therapeutic potential of modulating the ceramide/sphingomyelin pathway. J Clin Invest. 2002; 110:3–8. [PubMed: 12093880]
5. Kolesnick R, Hannun YA. Ceramide and apoptosis. Trends Biochem Sci. 1999; 24:224–225. [PubMed: 10366847]
6. Riboni L, Prinetti A, Bassi R, Caminiti A, Tettamanti G. A mediator role of ceramide in the regulation of neuroblastoma neuro2a cell-differentiation. J Biol Chem. 1995; 270:26868–26875. [PubMed: 7592930]
7. Cremesti AE, Goni FM, Kolesnick R. Role of sphingomyelinase and ceramide in modulating rafts: do biophysical properties determine biologic outcome? FEBS Lett. 2002; 531:47–53. [PubMed: 12401201]
8. Simons K, Ikonen E. Functional rafts in cell membranes. Nature. 1997; 387:569–572. [PubMed: 9177342]
9. Gulbins E, Dreschers S, Wilker B, Grassme H. Ceramide, membrane rafts and infections. J Mol Med. 2004; 82:357–363. [PubMed: 15069600]
10. Cremesti A, Paris F, Grassme H, Holler N, Tschopp J, Fuks Z, Gulbins E, Kolesnick R. Ceramide enables Fas to cap and kill. J Biol Chem. 2001; 276:23954–23961. [PubMed: 11287428]
11. Grassme H, Jekle A, Riehle A, Schwarz H, Berger J, Sandhoff K, Kolesnick R, Gulbins E. CD95 signaling via ceramide-rich membrane rafts. J Biol Chem. 2001; 276:20589–20596. [PubMed: 11279185]
12. Gulbins E, Kolesnick R. Raft ceramide in molecular medicine. Oncogene. 2003; 22:7070–7077. [PubMed: 14557812]
13. Junge S, Brenner B, Lepple-Wienhues A, Nilius B, Lang F, Linderkamp O, Gulbins E. Intracellular mechanisms of L-selectin induced capping. Cell Signal. 1999; 11:301–308. [PubMed: 10372808]
14. Goni FM, Alonso A. Biophysics of sphingolipids I. Membrane properties of sphingosine, ceramides and other simple sphingolipids. Biochim Biophys Acta. 2006; 1758:1902–1921. [PubMed: 17070498]
15. Sot J, Goni FM, Alonso A. Molecular associations and surface-active properties of short- and long-N-acyl chain ceramides. Biochim Biophys Acta. 2005; 1711:12–19. [PubMed: 15904658]

NIH-PA Author Manuscript

NIH-PA Author Manuscript

NIH-PA Author Manuscript

16. Bouwstra JA, Ponec M. The skin barrier in healthy and diseased state. Biochim Biophys Acta. 2006; 1758:2080–2095. [PubMed: 16945325]

17. Boulgaropoulos B, Arsov Z, Laggner P, Pabst G. Stable and Unstable Lipid Domains in Ceramide-Containing Membranes. Biophys J. 2011; 100:2160–2168. [PubMed: 21539783]

18. Chiantia S, Kahya N, Ries J, Schwille P. Effects of ceramide on liquid-ordered domains investigated by simultaneous AFM and FCS. Biophys J. 2006; 90:4500–4508. [PubMed: 16565041]

19. Goldschmidt-Arzi M, Shimoni E, Sabanay H, Futerman AH, Addadi L. Intracellular localization of organized lipid domains of C16-ceramide/cholesterol. J Struct Biol. 2011; 175:21–30. [PubMed: 21473916]

20. Holopainen JM, Lehtonen JYA, Kinnunen PKJ. Lipid microdomains in dimyristoylphosphatidylcholine-ceramide liposomes. Chem Phys Lipids. 1997; 88:1–13. [PubMed: 9297850]

21. Hsueh YW, Giles R, Kitson N, Thewalt J. The effect of ceramide on phosphatidylcholine membranes: A deuterium NMR study. Biophys J. 2002; 82:3089–3095. [PubMed: 12023232]

22. Huang HW, Goldberg EM, Zidovetzki R. Ceramide induces structural defects into phosphatidylcholine bilayers and activates phospholipase A(2). Biochem Biophys Res Commun. 1996; 220:834–838. [PubMed: 8607851]

23. Massey JB. Interaction of ceramides with phosphatidylcholine, sphingomyelin and sphingomyelin/cholesterol bilayers. Biochim Biophys Acta. 2001; 1510:167–184. [PubMed: 11342156]

24. Pandit SA, Chiu SW, Jakobsson E, Grama A, Scott HL. Cholesterol surrogates: A comparison of cholesterol and 16 : 0 ceramide in POPC Bilayers. Biophys J. 2007; 92:920–927. [PubMed: 17071659]

25. Silva L, De Almeida RFM, Fedorov A, Matos APA, Prieto M. Ceramide-platform formation and -induced biophysical changes in a fluid phospholipid membrane. Mol Membr Biol. 2006; 23:137–U132. [PubMed: 16754357]

26. Sot J, Bagatolli LA, Goni FM, Alonso A. Detergent-resistant, ceramide-enriched domains in sphingomyelin/ceramide bilayers. Biophys J. 2006; 90:903–914. [PubMed: 16284266]

27. Morrow MR, Helle A, Perry J, Vattulainen I, Wiedmer SK, Holopainen JM. Ceramide-1-Phosphate, in Contrast to Ceramide, Is Not Segregated into Lateral Lipid Domains in Phosphatidylcholine Bilayers. Biophys J. 2009; 96:2216–2226. [PubMed: 19289048]

28. Szoka F, Papahadjopoulos D. Comparative properties and methods of preparation of lipid vesicles (liposomes). Ann Rev Biophys Bioeng. 1980; 9:467–508. [PubMed: 6994593]

29. Berger O, Edholm O, Jahnig F. Molecular dynamics simulations of a fluid bilayer of dipalmitoylphosphatidylcholine at full hydration, constant pressure, and constant temperature. Biophys J. 1997; 72:2002–2013. [PubMed: 9129804]

30. Hess B, Kutzner C, van der Spoel D, Lindahl E. GROMACS 4: Algorithms for highly efficient, load-balanced, and scalable molecular simulation. J Chem Theo Comp. 2008; 4:435–447.

31. Shinoda W, Okazaki S. A Voronoi analysis of lipid area fluctuation in a bilayer. J Chem Phys. 1998; 109:1517–1521.

32. Pandit SA, Vasudevan S, Chiu SW, Mashl RJ, Jakobsson E, Scott HL. Sphingomyelin-cholesterol domains in phospholipid membranes: atomistic simulation. Biophys J. 2004; 87:1092–1100. [PubMed: 15298913]

33. Delaunay B. Sur la sphère vide. A la mémoire de Georges Voronoï. Bulletin de l'Académie des Sciences de l'URSS Classe des sciences mathématiques et na. 1934; 6:793–800.

34. Shewchuk JR. Delaunay refinement algorithms for triangular mesh generation. Computational Geometry-Theory and Applications. 2002; 22:21–74.

35. Dvinskikh SV, Castro V, Sandstrom D. Efficient solid-state NMR methods for measuring heteronuclear dipolar couplings in unoriented lipid membrane systems. PCCP. 2005; 7:607–613. [PubMed: 19787876]

36. Wu CH, Ramamoorthy A, Opella SJ. High-resolution heteronuclear dipolar solid-state NMR-spectroscopy. J Magn Reson, Ser A. 1994; 109:270–272.

37. Kucerka N, Liu YF, Chu NJ, Petrache HI, Tristram-Nagle ST, Nagle JF. Structure of fully hydrated fluid phase DMPC and DLPC lipid bilayers using X-ray scattering from oriented

NIH-PA Author Manuscript

NIH-PA Author Manuscript

NIH-PA Author Manuscript

multilamellar arrays and from unilamellar vesicles. Biophys J. 2005; 88:2626–2637. [PubMed: 15665131]

38. Shah J, Atienza JM, Duclos RI, Rawlings AV, Dong ZX, Shipley GG. Structural and thermotropic properties of synthetic C16-0 (palmitoyl) ceramide - effect of hydration. J Lipid Res. 1995; 36:1936–1944. [PubMed: 8558082]
39. Li L, Tang XP, Taylor KG, Dupre DB, Yappert MC. Conformational characterization of ceramides by nuclear magnetic resonance spectroscopy. Biophys J. 2002; 82:2067–2080. [PubMed: 11916863]
40. Huster D, Arnold K, Gawrisch K. Investigation of lipid organization in biological membranes by two-dimensional nuclear overhauser enhancement spectroscopy. J Phys Chem B. 1999; 103:243–251.
41. Thurmond RL, Dodd SW, Brown MF. Molecular areas of phospholipids as determined by H-2 NMR-spectroscopy - comparison of phosphatidylethanolamines and phosphatidylcholines. Biophys J. 1991; 59:108–113. [PubMed: 2015377]
42. Metcalf R, Pandit SA. Mixing Properties of Sphingomyelin Ceramide Bilayers: A Simulation Study. J Phys Chem B. 2012; 116:4500–4509. [PubMed: 22390271]
43. Quinn PJ. Lipid-lipid interactions in bilayer membranes: Married couples and casual liaisons. Prog Lipid Res. 2012; 51:179–198. [PubMed: 22342933]
44. Anishkin A, Sukharev S, Colombini M. Searching for the molecular arrangement of transmembrane ceramide channels. Biophys J. 2006; 90:2414–2426. [PubMed: 16415050]
45. Pascher I. Molecular arrangements in sphingolipids conformation and hydrogen-bonding of ceramide and their implication on membrane stability and permeability. Biochim Biophys Acta. 1976; 455:433–451. [PubMed: 999922]
46. Holopainen JM, Subramanian M, Kinnunen PKJ. Sphingomyelinase induces lipid microdomain formation in a fluid phosphatidylcholine/sphingomyelin membrane. Biochemistry. 1998; 37:17562–17570. [PubMed: 9860872]
47. Holopainen JM, Brockman HL, Brown RE, Kinnunen PKJ. Interfacial interactions of ceramide with dimyristoylphosphatidylcholine: Impact of the N-acyl chain. Biophys J. 2001; 80:765–775. [PubMed: 11159444]
48. Holopainen JM, Lemmich J, Richter F, Mouritsen OG, Rapp G, Kinnunen PKJ. Dimyristoylphosphatidylcholine/C16 : 0-ceramide binary liposomes studied by differential scanning calorimetry and wide- and small-angle X-ray scattering. Biophys J. 2000; 78:2459–2469. [PubMed: 10777742]
49. Nomura K, Lintuluoto M, Morigaki K. Hydration and Temperature Dependence of C-13 and H-1 NMR Spectra of the DMPC Phospholipid Membrane and Complete Resonance Assignment of Its Crystalline State. J Phys Chem B. 2011; 115:14991–15001. [PubMed: 22044314]

NIH-PA Author Manuscript

NIH-PA Author Manuscript

NIH-PA Author Manuscript

Highlights

- The interaction of C16-ceramide with DMPC bilayers has been studied.
- Solid-state NMR was used to verify predictions by MD simulations.
- The presence of C16-ceramide induces a higher order in the lipid bilayer.
- The interaction between lipid and ceramide is driven by specific H-bonds.

NIH-PA Author Manuscript

NIH-PA Author Manuscript

NIH-PA Author Manuscript

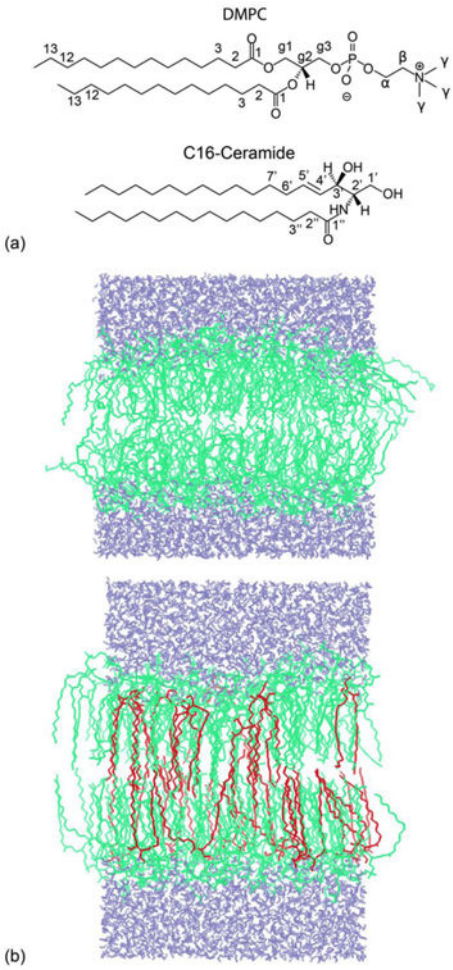

Fig. 1.

(a) Chemical structures of DMPC and C16-Ceramide. (b) Snapshots of the MD simulations of pure DMPC (top) and mixed DMPC/C16 (20%) bilayers (bottom), at 100 ns. The DMPC bilayer contained 128 lipid molecules (green) and 3655 water molecules (blue). The mixed DMPC/C16 bilayer contained 102 lipid molecules, 26 C16 molecules (red) and 3655 water molecules. C16 is fully incorporated into the DMPC bilayer. The temperature of the simulations was 310 K.

NIH-PA Author Manuscript

NIH-PA Author Manuscript

NIH-PA Author Manuscript

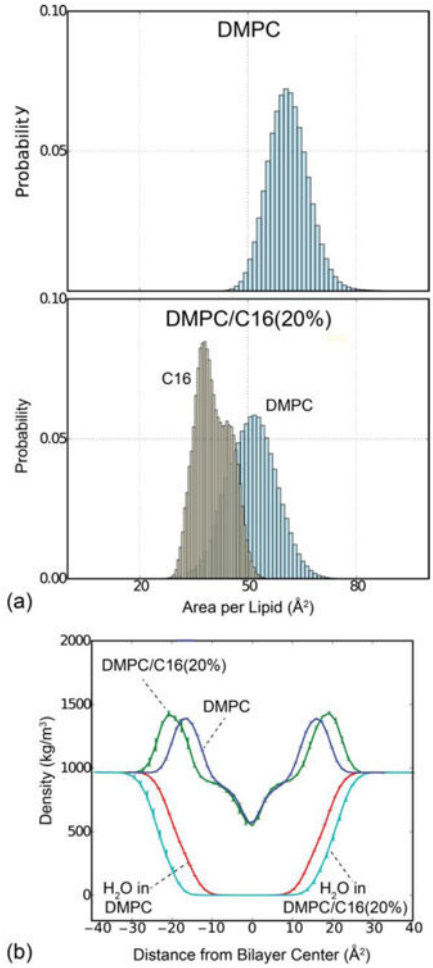

Fig. 2.

(a) Probability distribution of the area per lipid for pure DMPC (top) and DMPC/C16 mixtures (bottom). Within mixed bilayers, the area per DMPC is reduced to 51.0 ± 1.0 $Å^2$ in the presence of C16 compared to 61.1 ± 0.3 $Å^2$ for pure DMPC, as calculated by Voronoi analysis of MD simulation trajectories. (b) Mass density profiles along the perpendicular of the membrane plane for the complete systems (blue: DMPC, green: DMPC/C16) and for water only (red: DMPC, cyan: DMPC/C16). Total mass density profiles reveal a bilayer thickness of 32.3 ± 0.2 Å for DMPC, which is enlarged to 40.0 ± 0.4 Å in the presence of 20% C16. This change is reflected in the water density profile for both samples.

NIH-PA Author Manuscript
NIH-PA Author Manuscript
NIH-PA Author Manuscript

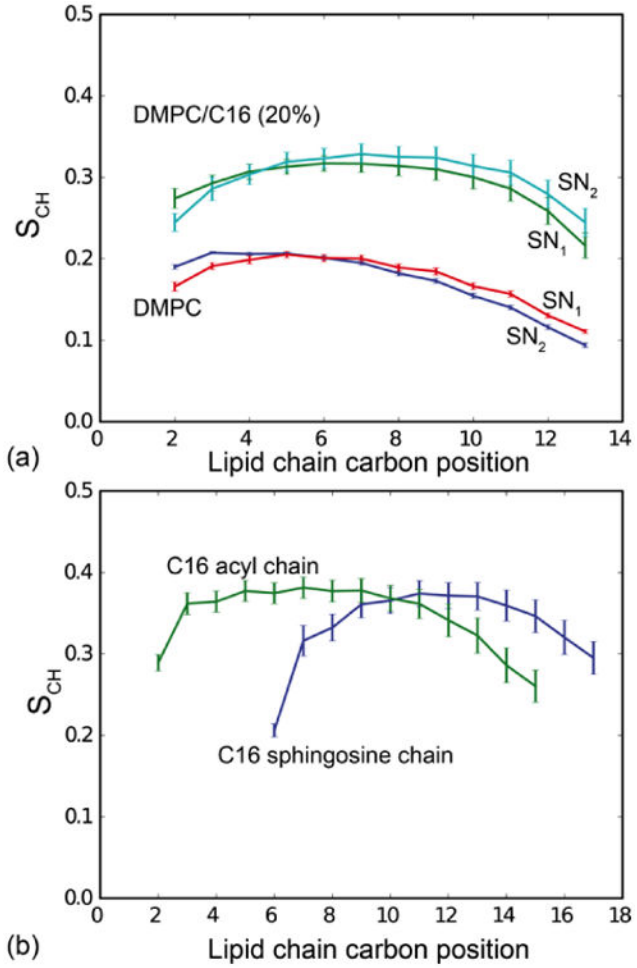

Fig. 3.

(a) Calculated segmental S_{CH} order parameters of DMPC alone and in the DMPC/C16 (20%) mixture. The simulations predict a significantly higher lipid order in the presence of C16-ceramide. (b) Calculated segmental S_{CH} order parameters of C16 in the DMPC/C16 (20%) mixture. The ceramide shows a slightly higher degree of order compared to DMPC in the mixture.

NIH-PA Author Manuscript
NIH-PA Author Manuscript
NIH-PA Author Manuscript

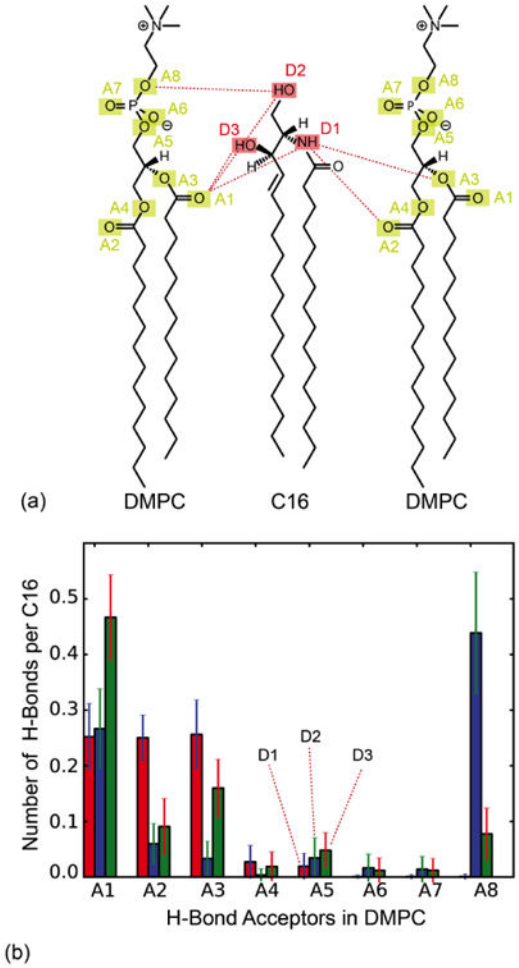

Fig. 4.

(a) Potential hydrogen-bond donors in C16-ceramide (D1-D3) and hydrogen-bond acceptors in DMPC (A1-A8). (b) Statistical analysis of H-bonds between DMPC and C16 observed in the simulated mixed bilayer, a snapshot of which is shown in Fig. 1b. The most likely H-bonds above a probability threshold of 0.2 are highlighted in (a).

NIH-PA Author Manuscript

NIH-PA Author Manuscript

NIH-PA Author Manuscript

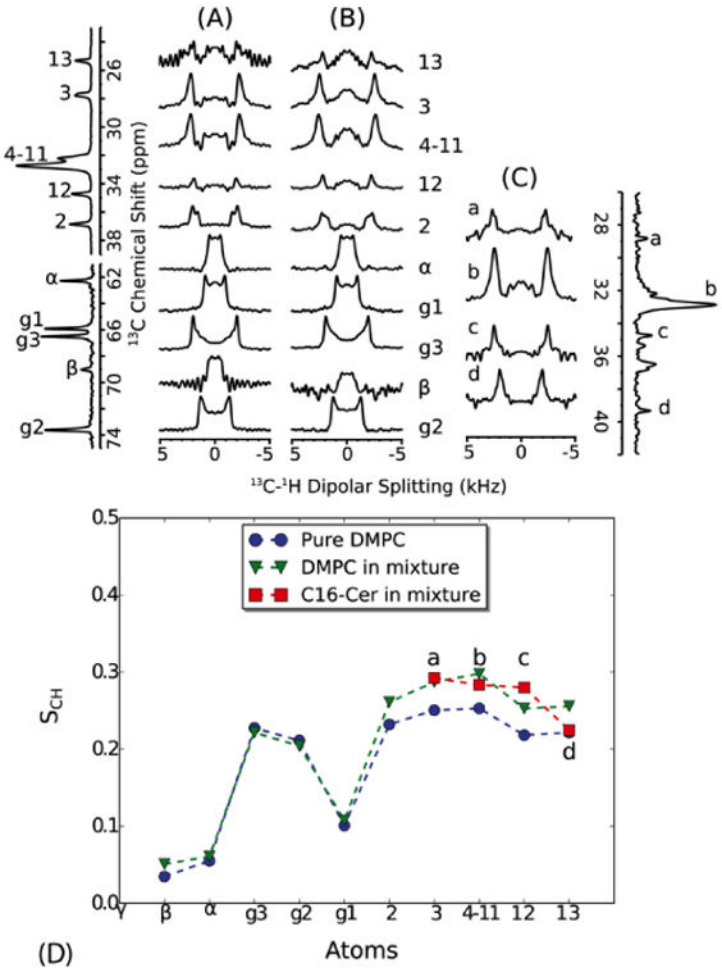

Fig. 5.

Dipolar C-H order parameters of DMPC were extracted from dipolar splittings obtained from pure DMPC (A) and from a mixture of DMPC/C16 (20%) (B). The order parameters of C16 were obtained from a sample of DMPC-d_{67}/C16 (20%) in which the ^{13}C-DMPC resonances show much reduced cross polarization intensities (C). The 1D spectra on the left and right are ^{13}C spectra of DMPC and DMPC-d_{67}/C16 (20%), respectively. The order parameters are plotted along the lipid carbon positions (D). Resonance b in C16 corresponds to the main CH_2 signal, but the other resonances are not assigned and are therefore plotted as "smoothed" order parameter profile in order of increasing chemical shift. Both C16 and DMPC show a similar degree of chain order, which is higher than pure DMPC. All spectra were recorded at 325 K. At this temperature, both C16 and DMPC are within a fluid phase within the mixture as judged from ^{1}H-MAS NMR spectra (Fig. 6). Dipolar couplings were calculated by dividing the dipolar splittings by the FSLG scaling factor (0.577 for CH and 0.816 for CH_2). Order parameters were calculated from the ratio of the measured dipolar couplings to the rigid single bond ^{13}C-^{1}H bond dipolar coupling (21.5 kHz [35]).

NIH-PA Author Manuscript

NIH-PA Author Manuscript

NIH-PA Author Manuscript

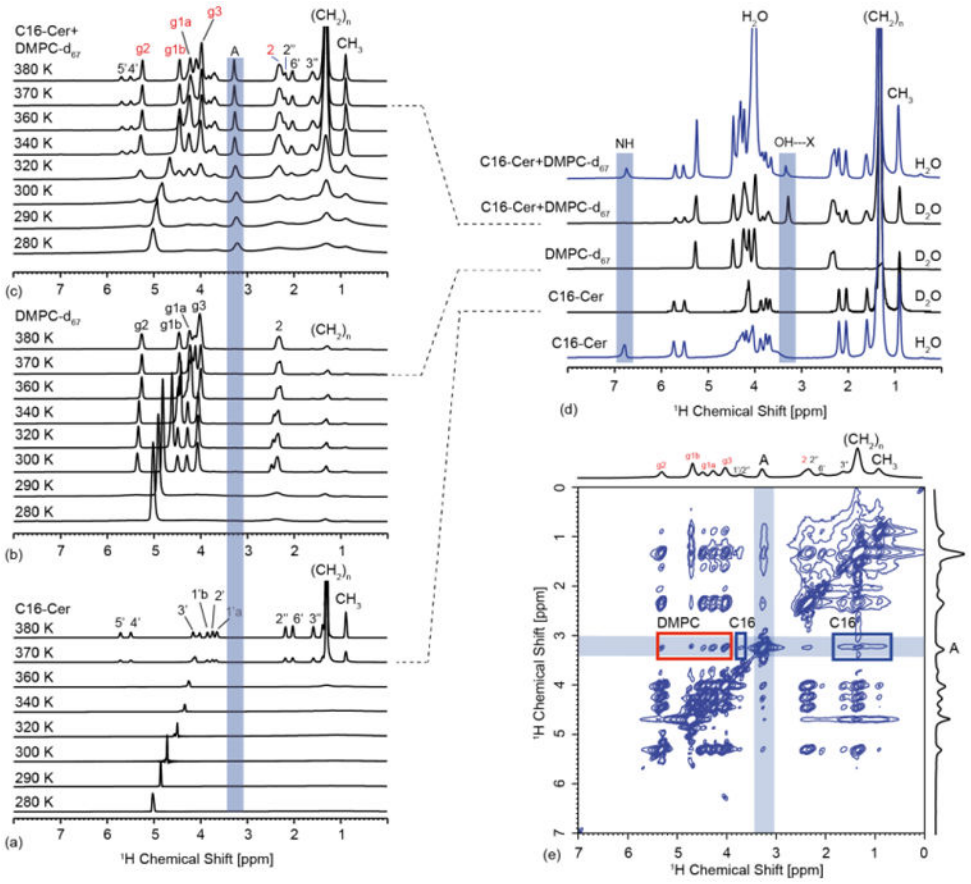

Fig. 6.

(a) Temperature dependent ^{1}H-MAS NMR spectra of C16 (a), DMPC-d_{67} (b) and DMPC-d_{67}/C16 (20%) (c). The main phase transition temperature of pure C16 as estimated from the $(CH_2)_n$ resonances is found around 370 K (a) but is lowered significantly to around 320 K in the mixture (c). This value is slightly above the phase transition of the lipids in the mixtures, which itself is elevated compare to pure DMPC (see Fig. S2). The proton spectrum of the mixture is in principle a superposition of lipid and C16 resonances, but one additional peak at 3.25 ppm, labelled 'A', appears (c). Comparing spectra in H_2O/D_2O reveals exchangeable sites such as the NH resonance (d). The peak A is tentatively assigned to the C16 OH proton involved in a H-bond with DMPC (see Fig. 4). (e) ^{1}H-MAS NOESY spectrum of DMPC-d_{67}/C16 (20%) in D_2O recorded at 310 K, 10 kHz sample rotation rate and a mixing time of 200 ms. At this temperature and mixing time, resonance A shows a number of cross peaks, with DMPC and C16 supporting our interpretation that A originates from 1-OH or 3-OH in C16 involved in a H-bond to DMPC. The C16 ^{1}H resonance assignment is based on solution-state NMR data for C18-ceramide and C16-dihydroceramide [39]. The assignment of DMPC is based on [49].

NIH-PA Author Manuscript
NIH-PA Author Manuscript
NIH-PA Author Manuscript

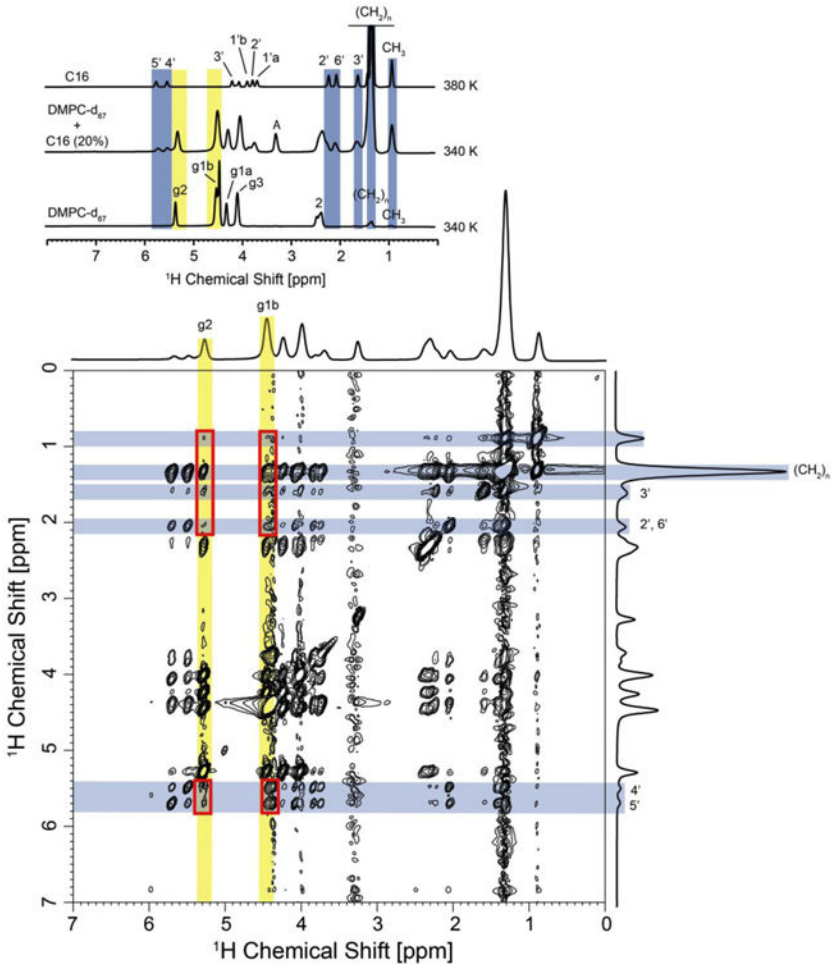

Fig. 7.

^{1}H-MAS NOESY spectrum of DMPC-d_{67}/C16 (20%) in D_2O recorded at 340 K, 10 kHz sample rotation rate and a mixing time of 1000 ms. An analysis of intermolecular DMPC – ceramide cross peaks was restricted to DMPC protons g2 and g1b, which show no overlap with ceramide proton resonances (see top insert). A number of intermolecular contacts have been observed, such as correlations between protons g2 and g3 in DMPC with protons CH_2, 3′, 2′, 6′, 4′ and 5′ in C16. Cross peaks are highlighted with red boxes. Unambiguously assigned lipid and C16 resonances are highlighted in yellow and blue, respectively.

NIH-PA Author Manuscript

NIH-PA Author Manuscript

NIH-PA Author Manuscript

Table 1

Summary of simulated trajectory analyses for DMPC and DMPC/C16; total bilayer area (in the XY plane), area per lipid, bilayer width (along Z-axis), and numbers of hydrogen-bonds. Note that a DMPC molecule has 9 potential hydrogen-bond acceptors and no donors. C16-ceramide has 3 potential donors and 4 potential acceptors (Fig. 4a).

	DMPC	**DMPC/C16 (20%)**
Membrane structure		
Total bilayer area (Å^2)	3956 ± 27	3151 ± 60
Area per lipid (Å^2)	61.1 ± 0.3	51.0 ± 1.0
Area per ceramide (Å^2)	-	40.3 ± 0.5
Bilayer width (Å)	32.3 ± 0.2	40.0 ± 0.4
Number of H-bonds		
DMPC - water per DMPC molecule	6.1 ± 0.1	5.6 ± 0.2
C16 - water per C16 molecule	-	0.9 ± 0.1
C16 - DMPC (total) per C16 molecule	-	2.6 ± 0.1
C16 (1-OH) - DMPC per C16 molecule	-	0.87 ± 0.06
C16 (3-OH) - DMPC per C16 molecule	-	0.88 ± 0.06
C16 (NH) - DMPC per C16 molecule	-	0.81 ± 0.05
C16-C16 (intra) per C16 molecule	-	0.06 ± 0.04
C16-C16 (inter) per C16 molecule	-	0.10 ± 0.04